7-1-2011

On Active Disturbance Rejection Based Control Design for Supercomputing RF Cavities

John Vincent
Michigan State University

Dan Morris
Michigan State University

Nathan Usher
Michigan State University

Zhiqiang Gao
Cleveland State University, Z.GAO@csuohio.edu

Shen Zhao
Cleveland State University

See next page for additional authors

Publisher's Statement

Original Citation

J. Vincent, D. Morris, N. Usher, Z. Gao, S. Zhao, A. Nicoletti and Q. Zheng, "On active disturbance rejection based control design for superconducting RF cavities," Nuclear Instruments and Methods in Physics Research Section A: Accelerators, Spectrometers, Detectors and Associated Equipment, vol. 643, pp. 11-16, 7/1, 2011.

Repository Citation

On active disturbance rejection based control design for superconducting RF cavities

John Vincent [a], Dan Morris [a], Nathan Usher [a], Zhiqiang Gao [b,*], Shen Zhao [b], Achille Nicoletti [b], Qinling Zheng [b]

[a] National Superconducting Cyclotron Laboratory (NSCL), Michigan State University, East Lansing, MI 48824-1321, USA
[b] Center for Advanced Control Technologies, Fenn College of Engineering, Cleveland State University, Cleveland, OH 44115-2214, USA

1. Introduction

The National Superconducting Cyclotron Laboratory (NSCL) is currently constructing a 3 MeV/u re-accelerator (ReA3), expandable to 12 MeV/u, using superconducting RF (SRF) cavities [1]. The project is cooperatively funded by the Michigan State University (MSU) and the National Science Foundation (NSF). In addition, MSU has been selected to build the Facility for Rare Isotope Beams (FRIB) national user facility that features a 400 kW, 200 MeV/u SRF linac requiring over 340 SRF cavities [2]. FRIB is funded through a cooperative agreement between MSU and the Office of Nuclear Physics in the Department of Energy (DOE) Office of Science. Maximizing the performance and decreasing the overall costs of these systems are the ongoing goals of both projects.

The control of lightly loaded SRF cavities is an ongoing topic in the accelerator community due to the extreme sensitivity of these cavities to disturbances and other detuning forces. A dominant method applied is to over-couple these cavities, thereby reducing the sensitivity by increasing the bandwidth and applying standard proportional-integral-derivative (PID) controls [3]. Adaptive control algorithms are sought that can minimize the required drive power and improve the overall performance of these systems. This paper describes our experience applying a seemingly ideal solution to this problem known as "Active Disturbance Rejection Control" (ADRC) [4,5].

The nature of many, if not most, control problems is disturbance rejection, particularly the microphonics problem discussed here, and the key question in design is how to deal with it. The PID control strategy, by default, deals with the disturbances in a passive way as it merely reacts to the tracking errors caused by the disturbances. An alternative, and better, solution is to reject the disturbances actively by estimating the disturbances directly and canceling it out, before it affects the system in a significant way, and this is at the core of ADRC.

In the ADRC design, the disturbance is estimated using the so called state observer, which is commonly used in the framework of modern control theory to estimate the immeasurable internal states of a system. Note that states, also known as state variables, refer to physical variables of a system, such as current, voltage, temperature, pressure, etc., and state observer, usually implemented in a computer algorithm, and uses the input and output data of a system, and its model, to reconstruct in real time the values of state variables [6].

The uniqueness of the ADRC design is that the total disturbance, which includes both external disturbances and unknown internal dynamics, is defined as an extended state of the system and estimated using a state observer, known as the extended state observer (ESO). Unlike the standard state observers, the state in ESO is extended beyond the regular physical variables to include the effects of unknown disturbance and dynamics in their totality. Once estimated, the total disturbance can be

readily canceled by the control signal, transforming elegantly the original system to a disturbance-free one, which can easily be controlled [4,5].

ARDC is practical because it requires very little knowledge about the plant dynamics, which in real systems may be both unknown and non-stationary. In the case of a linear time invariant system, it requires only the knowledge of the relative degree of the system and an estimation of the high frequency gain [5]. For example, given the general transfer function below (1), the information needed is the relative degree $n-m$ and b_m:

$$G(s)=\frac{b_m s^{(m)}+b_{m-1}s^{(m-1)}+\cdots+b_1 s+b_0}{s^{(n)}+a_{n-1}s^{(n-1)}+\cdots+a_1 s+a_0} \quad (1)$$

Additionally, the number of ARDC tuning parameters may be reduced to one [7], further simplifying the control design.

2. ADRC solution for the SRF cavity problem

In accelerator applications, the cavity voltage must be precisely controlled in the presence of vibrations referred to as "microphonics". The problem is acute here at NSCL since the ReA3 accelerator has been mounted on a balcony, making it even more susceptible to microphonic disturbances from the environment. The previously explored adaptive feedforward cancellation method [8] is found to be not sufficient in this case. We are thus motivated to explore more effective disturbance rejection technology beyond a standard PID and our search leads to ADRC. In this section the standard SRF cavity model [9] is first introduced, followed by a new problem formulation and the corresponding control design. Tuning of the new controller is also discussed.

2.1. Ideal voltage vector I–Q model

The cavity dynamics can be represented by a parallel RLC circuit as shown in Fig. 1, where $\vec{V}_c$ is the cavity voltage and $\vec{I}_g$ is the generator current.

According to Kirchhoff's law, we get the following second order differential equation:

$$\frac{d^2\vec{V}_c}{dt^2}+\frac{\omega_0}{Q}\frac{d\vec{V}_c}{dt}+\omega_0^2\vec{V}_c=\frac{R\omega_0}{Q}\frac{d\vec{I}_g}{dt} \quad (2)$$

where $\omega_0=1/\sqrt{LC}$ is the cavity resonant frequency and $Q=R\sqrt{C/L}$ is the quality factor.

For a fixed frequency RF system, transforming the cavity voltage and the driving current to a reference frame that rotates at the generator frequency ω_g, can greatly simplify the calculation [10]. The transformations are given below:

$$\vec{V}_c(t)=[V_{cI}(t)+jV_{cQ}(t)]e^{j\omega_g t} \quad (3)$$

$$\vec{I}_g(t)=[I_{gI}(t)+jI_{gQ}(t)]e^{j\omega_g t} \quad (4)$$

where V_{cI} and I_{gI} are the in-phase components and V_{cQ} and I_{gQ} are the quadrature components.

The amplitude of the cavity voltage and generator current are slowly changing compared to the RF component; thus $\dot{V}_c \ll \omega_g V_c$ and $\dot{I}_g \ll \omega_g I_g$. Together with $\omega_0 \approx \omega_g$ and $1/2Q \ll 1$, (2) can be simplified to the following two first-order differential equations:

$$\dot{V}_{cI}+\omega_{1/2}V_{cI}+\Delta\omega V_{cQ}=\omega_{1/2}V_{gI} \quad (5)$$

$$\dot{V}_{cQ}+\omega_{1/2}V_{cQ}-\Delta\omega V_{cI}=\omega_{1/2}V_{gQ} \quad (6)$$

where $\omega_{1/2}=\omega_0/2Q$ is the cavity half bandwidth; $\Delta\omega=\omega_0-\omega_g$ is the cavity detuning frequency; $V_{gI}\triangleq I_{gI}R$ and $V_{gQ}\triangleq I_{gQ}R$.

Note that the quadrature components in Eq. (5) and the in-phase components in Eq. (6) represent the coupling between the two channels, which is ignored in the existing PID design. This microphonic induced coupling is what makes the control design challenging for the SRF cavities.

2.2. Total disturbance rejection formulation and the corresponding ADRC design

The key problem in SRF cavity control is to maintain the constant amplitude and phase in V_c, which is a very challenging task as the resonant frequency ω_0 changes due to the Lorenz force and microphonics. Here the microphonics are part of external disturbances, denoted as d and the Lorenz force is field induced within the cavities and is a function of the system variable V_c. Therefore, the controller must mitigate both the external disturbances and the internal dynamics. Since the cavity resonant frequency $\omega_0(d,V_c)$ is actually a function of both the external disturbance (primarily microphonics) and the cavity voltage, a more realistic model of the cavity is

$$\dot{V}_{cI}+\omega_{1/2}V_{cI}+\Delta\omega(d,V_c)V_{cQ}=\omega_{1/2}V_{gI} \quad (7)$$

$$\dot{V}_{cQ}+\omega_{1/2}V_{cQ}-\Delta\omega(d,V_c)V_{cI}=\omega_{1/2}V_{gQ} \quad (8)$$

For such a nonlinear, time-varying and coupled system, the control design using regular methods could be very complicated. In the ADRC framework, however, all the nonlinear, time-varying and coupling terms are parts of the total disturbance to be estimated and mitigated, greatly simplifying the design task.

Considering the realistic model (7) and defining the output as $y=V_{cI}$, input as $u=V_{gI}$ and the total disturbance as $f=-\omega_{1/2}V_{cI}-\Delta\omega(d,V_c)V_{cQ}$, the in-phase component of the I–Q model can be reformulated as

$$\dot{y}=f+bu \quad (9)$$

where $b=\omega_{1/2}$. Now the task of ADRC comes down to a critical subtask: estimate f in real time. This is where the state observer from the modern control theory becomes a tool of choice. Define states as $x_1=y$ and $x_2=f$, where x_2 is called the extended state; thus Eq. (9) can be put into the matrix form as

$$\begin{bmatrix}\dot{x}_1\\ \dot{x}_2\end{bmatrix}=\begin{bmatrix}0 & 1\\ 0 & 0\end{bmatrix}\begin{bmatrix}x_1\\ x_2\end{bmatrix}+\begin{bmatrix}b\\ 0\end{bmatrix}u+\begin{bmatrix}0\\ 1\end{bmatrix}\dot{f}$$

$$y=x_1 \quad (10)$$

An ESO can be built to give the estimation of the states

$$\begin{bmatrix}\dot{z}_1\\ \dot{z}_2\end{bmatrix}=\begin{bmatrix}0 & 1\\ 0 & 0\end{bmatrix}\begin{bmatrix}z_1\\ z_2\end{bmatrix}+\begin{bmatrix}b\\ 0\end{bmatrix}u+\begin{bmatrix}\beta_1\\ \beta_2\end{bmatrix}(y-\hat{y})$$

$$\hat{y}=z_1 \quad (11)$$

where β_1 and β_2 are the observer gains.

A well-tuned observer in Eq. (11) provides the estimation of the total disturbance z_2, and the control law

$$u=\frac{-z_2+u_0}{b} \quad (12)$$

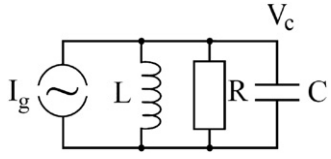

Fig. 1. Equivalent circuit model for cavity dynamics.

where u_0 is a virtual control signal, reduces the original plant in Eq. (9) to a simple integrator plant of the form

$$\dot{y} = u_0 + (f - z_2) \approx u_0 \quad (13)$$

which can be easily controlled using a proportional controller.

$$u_0 = k_p(r - z_1) \quad (14)$$

Here k_p is the controller gain and r is the reference signal.

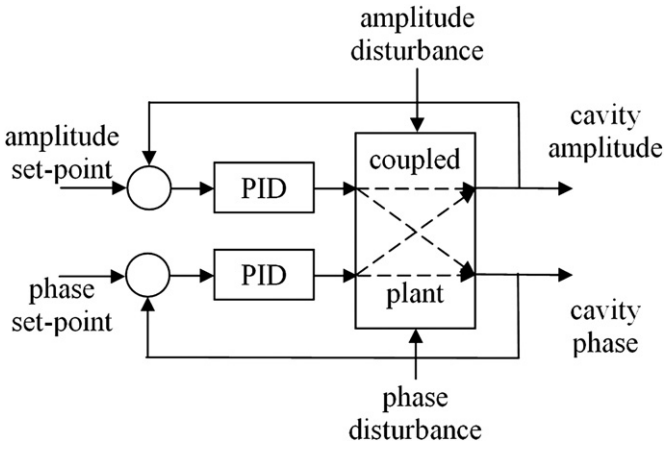

Fig. 2. Diagram of the PID control.

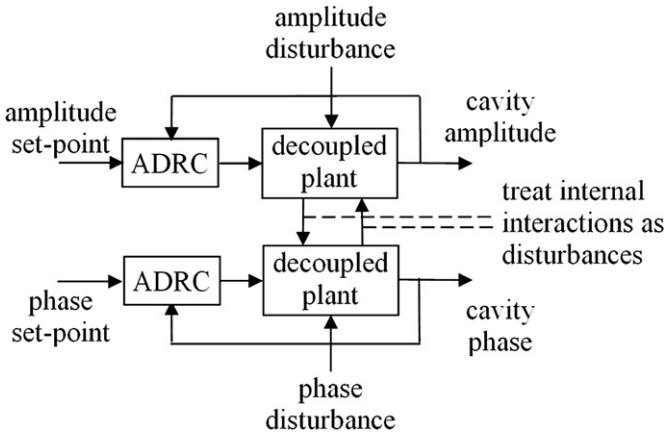

Fig. 3. Diagram of the ADRC control.

To simplify the tuning process, the observer gains are chosen as $\beta_1 = 2\omega_{ob}$ and $\beta_2 = \omega_{ob}^2$ to put the poles of the observer at $-\omega_{ob}$. Similarly the controller gains are chosen as $k_p = \omega_c$ to put the pole of the control loop at $-\omega_c$. ω_{ob} and ω_c are called the observer bandwidth and controller bandwidth, respectively. For further simplification, we can set $\omega_{ob} = (3-10)\omega_c$ and ω_c becomes the only tuning parameter [7].

The control design for the quadrature component can be carried out similarly by defining $y = V_{cQ}$, $u = V_{gQ}$ and $f = -\omega_{1/2} V_{cQ} + \Delta\omega(d, V_c)V_{cI}$.

2.3. Amplitude and phase control

As shown above, the cavity dynamics can be clearly described by the *IQ* model. However, in the real test environment, the electric field is normally measured in terms of amplitude and phase. The relationship between the *IQ* components and amplitude/phase is merely a linear coordinate transformation, from Cartesian to polar. For the sake of convenience and without loss of generality, the proposed ADRC solution is implemented to control the amplitude and phase directly instead of the *IQ* components, as the transformation does not affect the cavity dynamics. However a difficulty exists in phase control, since the phase can jump between -180° and 180°, which is referred to as the "wrap-around" problem. The problem is addressed in more detail in subsection D of Section III, while implementing the ADRC for phase loop.

Two diagrams are given in Figs. 2 and 3 to show the difference between the PID and ADRC for amplitude and phase control of the cavity, respectively. In a PID control structure, the amplitude and phase coupling, the disturbance and dynamic uncertainties are dealt with passively in the form of parameter tuning. In the ADRC design, however, they are lumped together as the total disturbance, estimated in real time, and actively canceled out in the corresponding control signal. In other words, another benefit of ADRC is that two coupled loops, such as the amplitude and phase loops in this application, are decoupled naturally.

3. Simulation and measured responses

3.1. Simulation model

A MATLAB simulation model is built to test the control design, as shown in Fig. 4. The cavity half bandwidth is 219 rad/s (35 Hz). The sampling rate is 54.6 kHz; the controller and observer

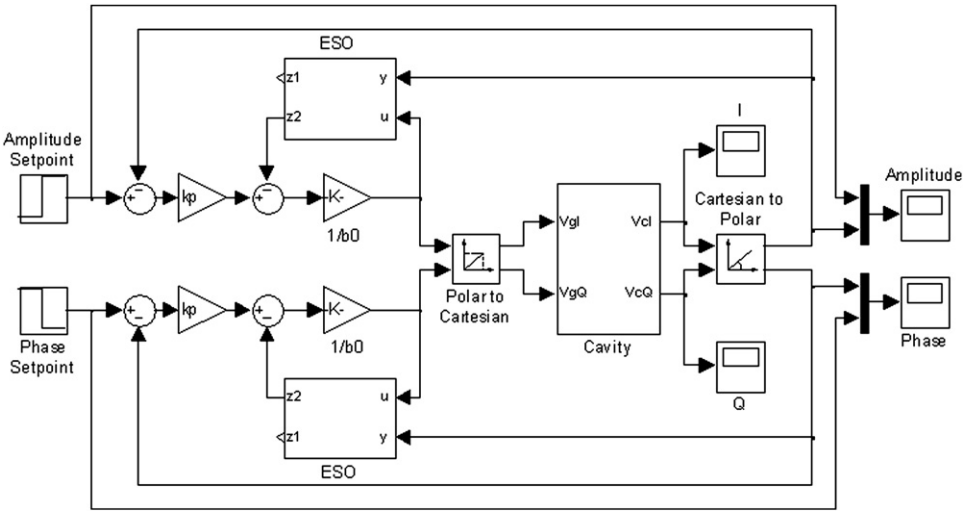

Fig. 4. MATLAB simulation model with ADRC control.

bandwidths are set to 600 and 3000 rad/s, respectively. For comparison, a PI controller is tuned with a proportional gain of 3 and an integral gain of 5474. The parameters were tuned to achieve the best stable response. The same values were used for simulations and measurements.

3.2. Hardware implementation

The RF control is implemented on a digital low-level RF controller developed at the NSCL. The controller produces a low-level RF output at the cavity drive frequency and directly controls the phase and amplitude of the output. This low-level RF signal is fed into a solid-state linear amplifier and the output of the amplifier is coupled to the cavity. The cavity used for these tests is a SRF quarter wave resonator with a loaded bandwidth of 70 Hz (440 rad/s). This particular cavity is especially susceptible to microphonics because its mechanical damper does not work as well as anticipated. During the tests, intermittent microphonics were present, which detuned the cavity by more than 40 Hz. The discrete implementation of the ADRC control algorithm can be found in Ref. [11].

3.3. Simulation and measured results

Step signals were introduced as a reference for both the amplitude and phase components. For the simulations, a constant detuning frequency of 40 rad/s was used. The simulated and measured response curves for a step in amplitude (6→8 MV/m) are shown in Fig. 5. The response curves for a step in phase (75→90°) are shown in Fig. 6. With the ADRC controller, the ripple and overshoot are greatly reduced.

The steady-state probability density functions for amplitude and phase are shown in Fig. 7. The steady-state model includes a Gaussian detuning frequency, which was varied in order to match the measured data.

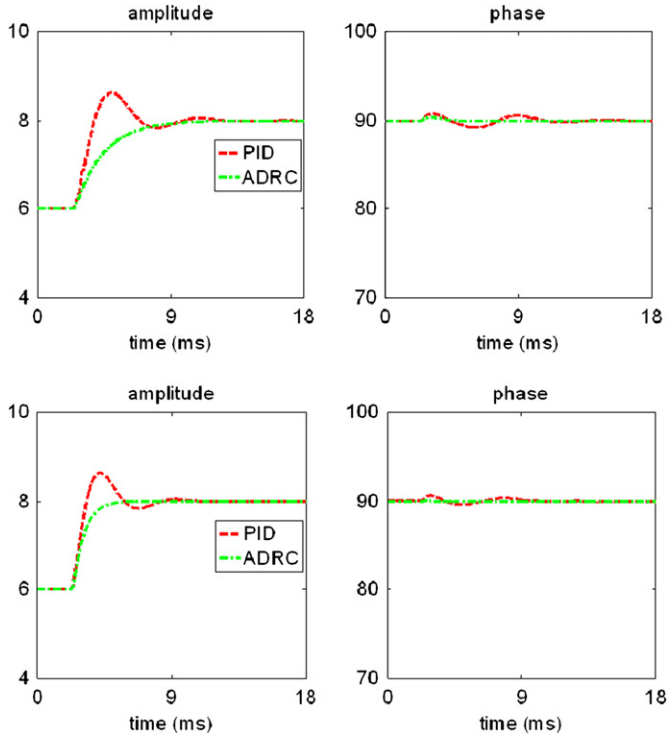

Fig. 5. Amplitude step response: simulation (top) and measured (bottom).

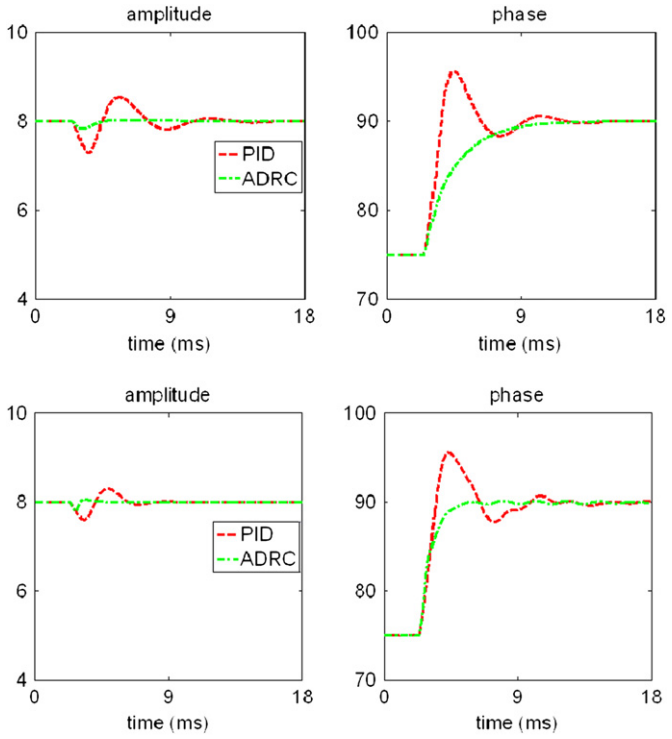

Fig. 6. Phase step response: simulation (top) and measured (bottom).

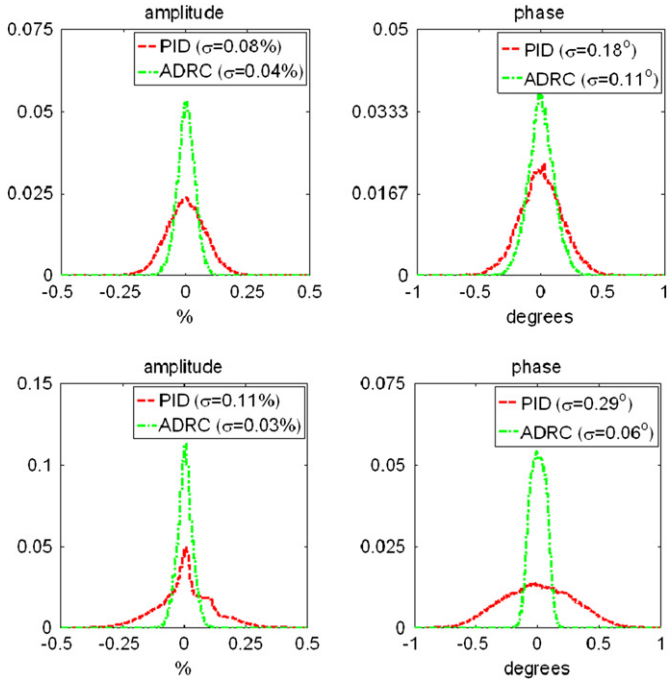

Fig. 7. Steady-state probability density function: simulation (top) and measured (bottom).

3.4. Implementation issues

Physical limitations always exist for the actuators. For example, in the amplitude loop, the output voltage of the amplifier is limited to 0–10 V, which results in a difference between the actual applied and the calculated control signal. In the observer based design, the control signal is needed for the state estimation. Normally feeding back the control signal that is actually applied

on the real system to the observer will give us a more accurate estimation. It works very well with the amplitude loop.

In the phase loop, however, feeding back the actual applied control signal gives us unexpected results. The phase output cannot get to the setpoint in some special cases. A simulation example for the case is shown in Fig. 8.

The reason for it is that the phase loop is different from the amplitude loop in the sense of how the control signal is handled due to the physical limitation. In the amplitude loop, the control signal is saturated between a lower bound and an upper bound. In the phase loop, the 270° control signal will have the same effect as that of −90° control signal. So a wrap-around method is used instead of the saturation method. In the wrap-around method, whenever the control signal goes beyond the range from −180° to 180°, 360° is added to or subtracted from the control signal to make it fall back into this range. The effect of the saturation and wrap-around is graphed in Figs. 9 and 10. It is the non-monotonic behavior of the phase loop that causes the multi-equilibrium points of the system, and hence the above problem.

To solve the problem, we first tried the saturation method for the phase loop to avoid the non-monotonic behavior, but it did not work. The phase saturates at either the upper limit or the lower limit and cannot recover from the saturation point. This is because naturally the phase can approach its setpoint in both directions. In the saturation method, we manually block one of the directions. So once the phase initially goes in the wrong direction, it will always saturate.

So we switched back to the wrap-around method that preserves the feature of the phase behavior. We finally solved the problem in simulation by feeding back the calculated control

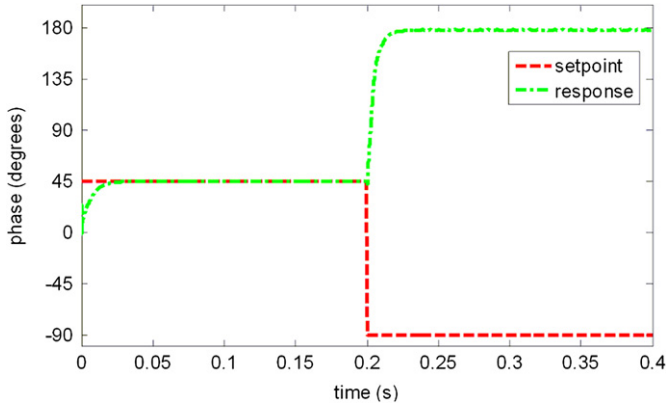

Fig. 8. Undesired response for phase loop.

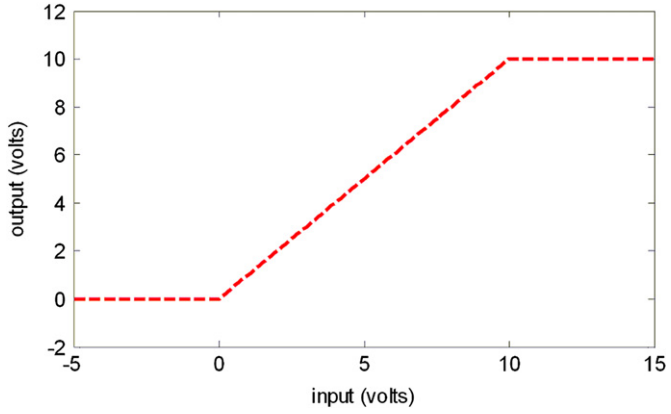

Fig. 9. Saturation effect for amplitude loop.

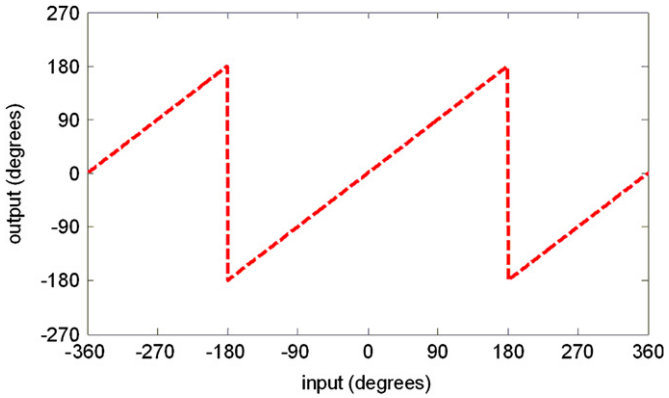

Fig. 10. Wrap-around effect for phase loop.

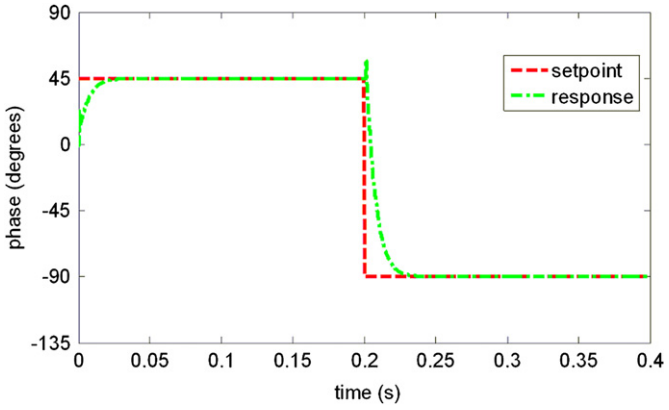

Fig. 11. Desired response for phase loop.

signal (before the wrap-around) instead of the actually applied control signal (after the wrap-around) to the ESO. In this way we actually consider the wrap-around effect (adding or subtracting 360° to or from the calculated control signal) as an input disturbance, and use the disturbance rejection ability of the ADRC to deal with it. A simulation result is given in Fig. 11 to show the effectiveness of this method.

The new wrap-around implementation has been tested on several superconducting cavities, and it solves the problems found in the previous implementations. When running the new design, large disturbances do not cause control problems and the phase setpoint can be changed arbitrarily without causing the saturation problem illustrated in Fig. 8.

4. Conclusion

The initial tests of the ADRC control on a SRF cavity at the NSCL have shown a significant improvement over the PID control under the same conditions. We expect that as we continue to work with the implementation, we may improve the response even further.

Acknowledgments

This work was supported in part by the National Science Foundation under Grant no. PHY-06-06007.

References

[1] Oliver Kester, et al., The MSU/NSCL re-accelerator ReA3, in: Proceedings of the SRF2009, Berlin, Germany, 2009, pp. 57–61.

[2] R.C. York, et al., FRIB: a new accelerator facility for the production of rare isotope beams, in: Proceedings of the SRF2009, Berlin, Germany, 2009, pp. 888–894.
[3] Curt Hovater, RF control of high QL superconducting cavities, in: Proceedings of the LINAC08, Victoria, BC, Canada, 2008, pp. 704–708.
[4] Z. Gao, Active disturbance rejection control: a paradigm shift in feedback control system design, in: Proceedings of the American Control Conference, 2006, pp. 2399–2405.
[5] J. Han, IEEE Transactions on Industrial Electronics 56 (3) (2009) 900.
[6] P.J. Antsaklis, A.N. Michel, Linear Systems, McGraw-Hill Companies Inc., 1997.
[7] Z. Gao, Scaling and bandwidth-parameterization based controller tuning, in: Proceedings of the American Control Conference, 2003, pp. 4989–4996.
[8] T.H. Kandil, et al., Nuclear Instruments & Methods in Physics Research Section A 550 (2005) 514.
[9] S. Simrock, G. Petrosyan, A. Facco, V. Zviagintsev, S. Andreoli, R. Pa-parella, First demonstration of microphonic control of a superconducting cavity with a fast piezoelectric tuner, in: Proceedings of the 2003 Particle Accelerator Conference, Portland, OR, 2003, pp. 470–472.
[10] M.G. Minty, R.H. Siemann, Nuclear Instruments and Methods in Physics Research Section A 376 (1996) 310.
[11] R. Miklosovic, A. Radke, Z. Gao, Discrete implementation and generalization of the extended state observer, in: Proceedings of the American Control Conference, 2006, pp. 2209–2214.